

ANALYSIS OF A WIRE IN THE PRESENCE OF AN OPEN BODY OF REVOLUTION

Z. Qiu and C. M. Butler

- 1. Introduction**
 - 2. Formulation**
 - 3. Results**
- Acknowledgements**
References

1. Introduction

In this paper we consider the problem of a wire in the presence of a hollow body of revolution (*BOR*). The geometry of the wire/*BOR* configuration is depicted in Figure 1, where one sees a hollow *BOR* with a circular aperture at the top of the hollow body. The plane of the aperture is parallel to the xy plane and the wire can be located inside the body, outside the body, or partially inside and partially outside. In special cases, the wire can be mounted on the body. The configuration depicted in Figure 1 is representative of many practical situations.

The coupling between a wire antenna and general bodies of revolution has been treated by several investigators [1–10]. Glisson and Butler [1] have analyzed an arbitrarily-oriented, thin-wire antenna located near a *BOR*, but not attached to it, by a method incorporating a numerical Green's function. Newman and Pozar [2] used the sinusoidal reaction method to solve the integral equation for the current on composite wire and surface structures. Shaeffer and Medgyesi-Mitschang [3,4] have investigated a thin wire attached to a *BOR* by introducing a special junction basis function. Richmond [5] treated a thin wire attached to a circular disk, and Perez-Leal and Catedra have determined

the input impedance of a thin wire attached on-axis to a conducting *BOR* and fed at the attachment point [6]. For a dipole mounted on a cylinder, Tsai [7] developed a model which depends on the determination of the elements of an array of magnetic ring sources. Yung and Butler [8] studied the interaction between the radiating portion of the antenna and its feed system, and a hybrid technique, based on the method of moments and the geometric theory of diffraction, has been used to investigate the input impedance of a monopole located on a disk [9,10].

The coupling between the wire and the body has not been studied for the case where the wire is located partially inside the *BOR* shell and partially outside, and the full mode current on the two conductors has not been reported to date. In this paper, a technique is presented for modeling a wire antenna in the presence of a *BOR*, including the case where the wire is attached to the *BOR* surface. The total electric current induced on the wire and *BOR* is computed for different types of excitation, including antenna sources and incident plane waves. Full account is taken of the coupling between the wire and *BOR*, including the effects of the wire-to-*BOR* and *BOR*-to-wire coupling for all Fourier modes. The technique is based on the *BOR* theory alone and the wire and *BOR* are treated as either parts of a whole body of revolution or as two constituent parts of a composite body. In addition, the wire is not restricted to be thin. For the special case that a wire probe is mounted on the cap of a cylinder, the input admittance is measured and computed. Good agreement between measurements and numerical results is obtained.

2. Formulation

Figure 1 illustrates a wire in the presence of a hollow body of revolution. The wire can be located inside, outside, or partially inside and partially outside the hollow *BOR*. Both the wire and *BOR* are perfect conductors (*pec*) and the *BOR* is considered to have a vanishingly thin (shell) wall. They share a common axis and are treated as a composite body of revolution whose generating arc comprises that of the wire and that of the *BOR*. As usual, the body of revolution is generated by rotating its composite arc through 2π radians about its axis.

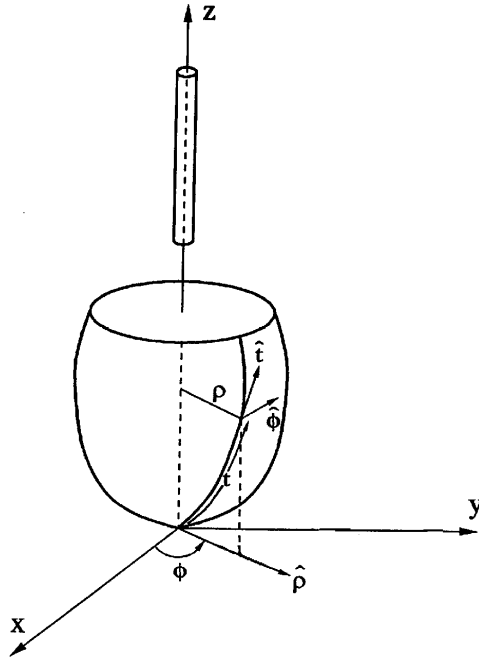


Figure 1. A wire in the presence of a hollow body of revolution.

Coupled integral equations for the Fourier coefficients of the electric current induced on the wire and *BOR* are given in Appendix A. To solve these equations, one can expand the Fourier coefficients of the t -directed currents (times ρ) $\rho J_m^{t,wire}$ and $\rho J_m^{t,BOR}$ (see Figure 1) on the wire and *BOR*, respectively, as linear combinations of known basis functions. Instead of expanding $J_m^{t,wire}$ and $J_m^{t,BOR}$ directly, the coupled integral equations are simplified somewhat, if

$$\rho(t) J_m^{t,wire}(t) = \sum_{n=1}^{N_{t1}} \mathcal{J}_{n,w}^{t,m} \Lambda_n(t) \quad (1a)$$

$$\rho(t) J_m^{t,BOR}(t) = \sum_{n=1}^{N_{t2}} \mathcal{J}_{n,b}^{t,m} \Lambda_n(t), \quad (1b)$$

where $\mathcal{J}_{n,w}^{t,m}$ and $\mathcal{J}_{n,b}^{t,m}$ are unknown coefficients, N_{t1} and N_{t2} are the numbers of unknowns on the wire and *BOR*, respectively. The

generating arc is approximated by an arc comprising piecewise straight-line segments joining points designated $\dots, n-1, n, n+1, \dots$ that fall on the original arc. $\Lambda_n(t)$ is a triangle function defined on the generating arc in the usual way:

$$\Lambda_n(t) = \begin{cases} \frac{t - t_{n-1}}{\Delta_{n-1/2}} & , t \in (t_{n-1}, t_n) \\ -\frac{t - t_{n+1}}{\Delta_{n+1/2}} & , t \in (t_n, t_{n+1}). \\ 0 & , \text{otherwise} \end{cases} \quad (2)$$

where t_{n-1} , t_n , and t_{n+1} are the arc displacements measured from the reference at $t = 0$ to the $(n-1)^{th}$, n^{th} , and $(n+1)^{th}$ points on the original generating arc. The lengths of the straight-line segments joining points $n-1$ to n and points n to $n+1$ are designated $\Delta_{n-1/2}$ and $\Delta_{n+1/2}$, respectively.

The Fourier coefficients $J_m^{\phi, wire}$ and $J_m^{\phi, BOR}$ of the ϕ -directed currents on the wire and BOR are expanded in pulses as

$$J_m^{\phi, wire}(t) = \sum_{n=1}^{N_{\phi 1}} \mathcal{J}_{n,w}^{\phi,m} \Pi_{n-1/2}(t) \quad (3a)$$

$$J_m^{\phi, BOR}(t) = \sum_{n=1}^{N_{\phi 2}} \mathcal{J}_{n,b}^{\phi,m} \Pi_{n-1/2}(t) \quad (3b)$$

where $\mathcal{J}_{n,w}^{\phi,m}$ and $\mathcal{J}_{n,b}^{\phi,m}$ are unknown coefficients and $N_{\phi 1}$ and $N_{\phi 2}$ are the numbers of unknowns on the wire and BOR, respectively. $\Pi_{n-1/2}$ is a pulse function defined by

$$\Pi_{n-1/2}(t) = \begin{cases} 1 & , t \in (t_{n-1}, t_n) \\ 0 & , \text{otherwise.} \end{cases} \quad (4)$$

If the wire is attached to the BOR, the t -directed and ϕ -directed current on the wire and BOR can be simply expressed as

$$\rho(t) J_m^t(t) = \sum_{n=1}^{N_t} \mathcal{J}_n^{t,m} \Lambda_n(t) \quad (5)$$

and

$$J_m^\phi(t) = \sum_{n=1}^{N_\phi} \mathcal{J}_n^{\phi,m} \Pi_{n-1/2}(t) \quad (6)$$

where N_t and N_ϕ are the numbers of unknown coefficients of the t -directed and ϕ -directed currents on the wire and BOR . We test the t -directed electric field equation by means of pulse functions

$$T_q^t(t) = \Pi_q(t) \quad (7)$$

To test the ϕ -directed field equation, we choose point-matching:

$$T_q^\phi(t) = \delta(t - t_{q-1/2}), \quad (8)$$

where $t_{q-1/2}$ is the mid point of segment q .

An impedance matrix is formed and the expansion coefficients in (1), (3), (5) and (6) are computed by the usual moment method procedure. The excitation can be an incident plane wave or a voltage source. The incident electric field is assumed to be of the form

$$\mathbf{E}^i(\rho, \phi, z) = E^{inc} \hat{\theta}(\theta^i, \phi^i) \cdot e^{jk(\rho \sin \theta^i \cos(\phi - \phi^i) + z \cos \theta^i)} \quad (9)$$

where E^{inc} is the magnitude of the field, and θ is the angle between the z axis and the ray from the origin to the observation point. ρ, ϕ, z are cylindrical coordinate variables.

To determine the input admittance of a coax-fed wire attached to the BOR , one excites the wire by the field which penetrates the coaxial aperture. To model this coaxial source, one appeals to the equivalence theorem. The aperture is shorted and an appropriate surface magnetic current is impressed on this resulting conducting surface. The field from this magnetic frill current in free space is given by Butler and Tsai [11]. With this source, one can solve the coupled integral equations for the electric current on the wire and determine the input admittance of the wire antenna as the ratio of the electric current at this feed point and the voltage across the coaxial aperture. The far-field radiation pattern can be calculated by integrating the electric current on the wire and BOR against the far-zone, free-space Green's function:

$$E_\theta = \frac{2\pi k \eta}{4\pi r} e^{-jkr} (F_1(\theta) + F_2(\theta)) \quad (10)$$

where

$$F_1(\theta) = \int_0^L \rho(t') J_t(t') (\hat{\rho}' \cdot \hat{t}') \cos \theta e^{jkr' \cos \theta \cos \theta'} J_1(kr' \sin \theta \sin \theta') dt' \quad (11a)$$

and

$$F_2(\theta) = j \int_0^L \rho(t') J_t(t') (\hat{z} \cdot \hat{t}') \sin \theta e^{jkr' \cos \theta \cos \theta'} J_0(kr' \sin \theta \sin \theta') dt' \quad (11b)$$

in which $J_t(t)$ is the t -directed electric current on the wire and BOR and L is the total length of the wire and generating arc of the BOR . $J_0(\cdot)$ and $J_1(\cdot)$ are the zero and first order Bessel functions.

3. Results

In this section, we present and discuss data obtained from solutions of the integral equations mentioned above and in the appendix. Also, in the case of selected configurations, we report experimental results obtained from measurements made on laboratory models. The experimentally-determined data serve to corroborate those obtained from the theoretical/numerical techniques. Several configurations of interest are treated.

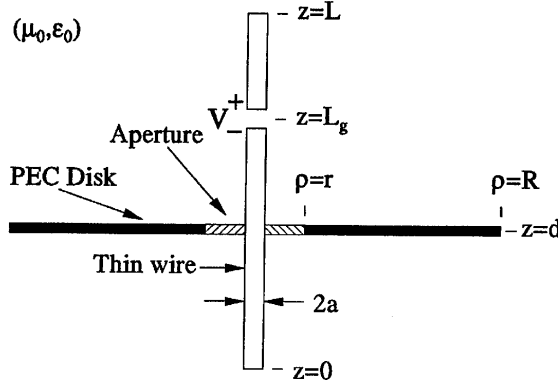


Figure 2. A cross-sectional view of thin-wire antenna located in a circular aperture at the center of a circular disk.

A cross-sectional view of a thin-wire antenna located in a circular aperture at the center of a circular disk is presented in Figure 2. The antenna, perpendicular to the plane of the disk, is of length $L = 1.5\lambda$ (λ being wavelength) and radius $a = 0.001\lambda$ and is excited by a voltage source located at a displacement of $z = L_g = 1.125\lambda$ from the lower end of the wire. The disk and aperture radii are $R = 10\lambda$ and $r = 0.1\lambda$, respectively.

In Figure 3a is depicted the current on the thin-wire antenna of Figure 2 in free space (no circular disk), which is excited by a one-volt slice generator. In Figure 3b is shown the current on the same wire subject to the same excitation as in Figure 3a, except in this case the disk is returned at the wire center ($d = 0.75\lambda$). One observes from Figure 3a and Figure 3b that the currents in the two cases are almost the same, which implies that the *pec* disk has virtually no effect on the wire current as one expects, because the disk is located at a position corresponding to a zero derivative of electric current where the radial electric field due to the wire current is zero or small. With the disk located at $z = d = 0.375\lambda$ where the current has a large derivative, corresponding to a position of large charge density, it has a strong influence on the wire current as can be seen by a comparison of the current presented in Figure 3c with that presented in Figure 3b. The values of the current distributions of Figures 3b and 3c on the wire through the hole in the large conducting disk are very close to those on the wire through the hole in a *pec* screen reported by Butler and Martin [12]. The influence of a circular disk having large diameter to wavelength ratio on the current on a wire through its center hole is essentially the same as that of a *pec* screen on the current on a wire through a hole in such a screen. The radial electric field normal to the wire surface is parallel to the surface of the *pec* disk and, hence, interacts with the disk. Because this electric field is proportional to the charge on the wire or, equivalently, to the derivative of the wire current, one does expect the presence of the disk at a location of rapidly changing current, i.e., large derivative, to strongly influence the wire current, as is observed to be the case in the data presented here. On the other hand, as is evident from Figure 3, when the disk is located at a point where the derivative is small, it has little influence on the wire current.

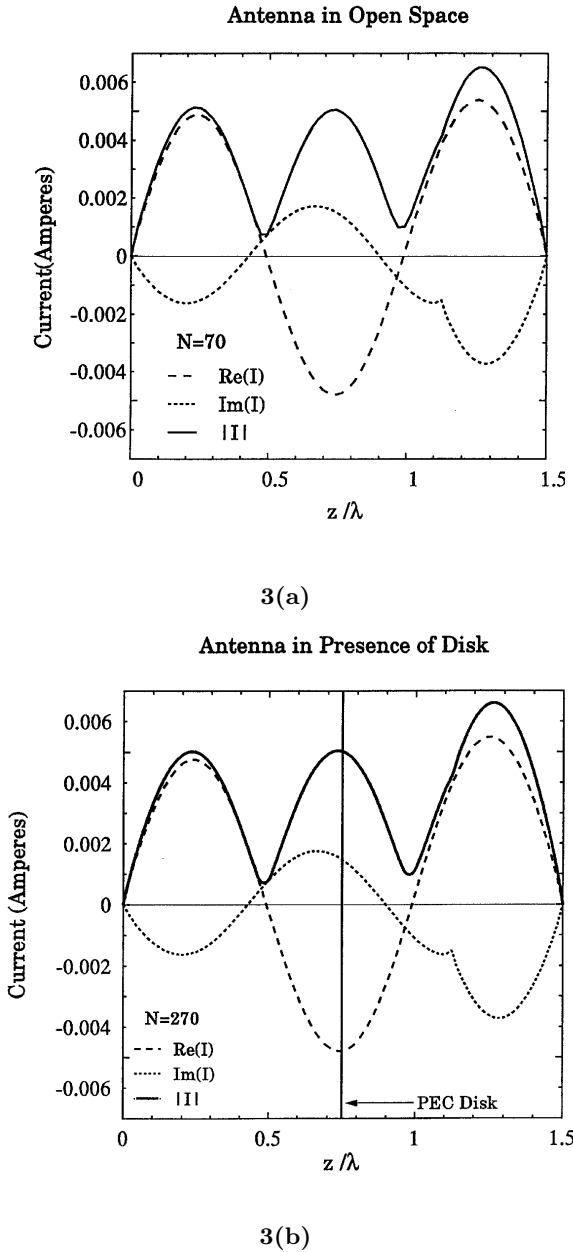
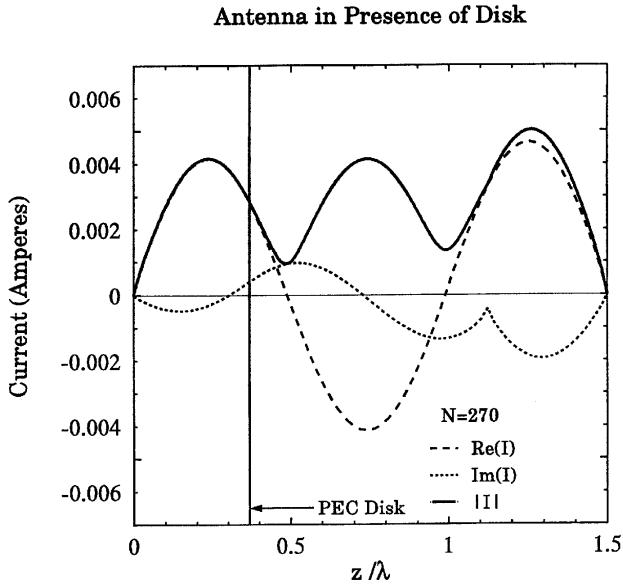


Figure 3. Current distribution on a thin-wire antenna ($L/\lambda = 1.5$, $a/\lambda = 0.001$, $L_g/\lambda = 1.125$, $V=1$ volt). (a) no PEC Disk, (b) PEC Disk at $d/\lambda = 0.75$, $R/\lambda = 10$ and $r/\lambda = 0.1$.



3(c)

Figure 3. Current distribution on a thin-wire antenna ($L/\lambda = 1.5$, $a/\lambda = 0.001$, $L_g/\lambda = 1.125$, $V=1$ volt). (c) PEC Disk at $d/\lambda = 0.375$, $R/\lambda = 10$ and $r/\lambda = 0.1$.

In Figure 4 is an illustration of a wire in the presence of a hollow tube with closed bottom and open top, with the two bodies sharing a common axis. The wire is of length $L = 0.3\lambda$ and radius $b = 0.01\lambda$, and the thin-wall “cup” is of height $H = 0.5\lambda$ and radius $a = 0.125\lambda$. The excitation is an incident plane wave (Eq. (9)). The total t -directed and ϕ -directed electric currents on the cup, normalized with respect to the magnitude of the incident magnetic field (H^{inc}) times $(1/\eta)$ (see figures), are shown in Figure 5 for the case in which the wire is located outside the cup ($s > H$). Since the two components of current are dependent upon ϕ , these data are presented as families of curves of current for selected discrete values of ϕ around the cup. Notice that the total t -directed and ϕ -directed currents on the cup are functions of ϕ and t and that the ϕ -directed current approaches infinity at the edges of the cup. However, the total electric current on the *wire* depends only slightly on ϕ and the ϕ -directed current is approximately zero, or is very small compared to that in the t direction, except at the two edges,

as is seen in Figure 6. The lower end of the wire for the data of Figure 6 is at $z = 1\lambda$ and the upper at $z = 1.3\lambda$. The currents of Figures 7 and 8 are for the case that the wire is partially inside and partially outside the cup ($s = 0.35\lambda$), with the lower end of the wire now at $z = 0.35\lambda$ and the upper end outside the cup at $z = 0.65\lambda$. One observes from Figures 5 and 7 that the cup currents are essentially the same for the different wire locations, even though, as seen in Figures 6 and 8, the wire currents are quite different. Hence, one concludes that the wire to cup coupling is weak, i.e., the influence of the wire current on the cup current is small.

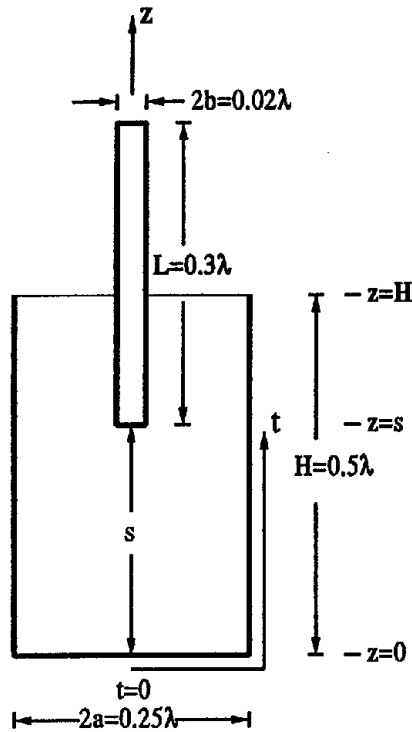


Figure 4. A cross-sectional view of a thin-wire in the presence of a cup.

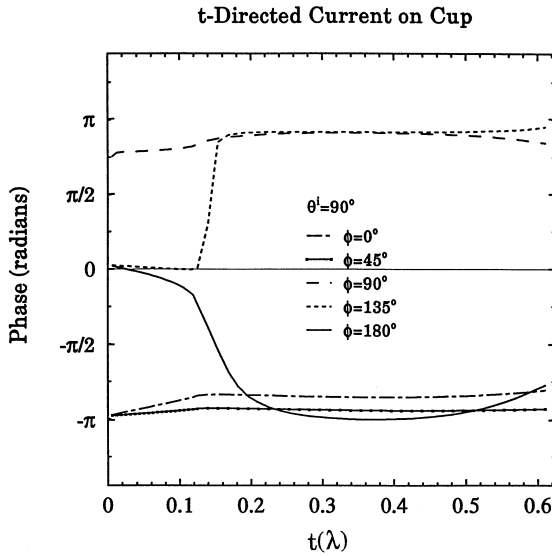
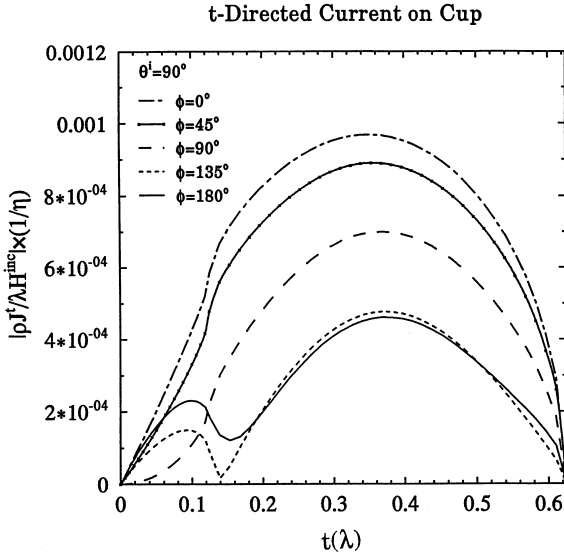


Figure 5. Current distribution on a cup near a wire due to an incident plane wave($a/\lambda=0.125$, $H/\lambda=0.5$, $b/\lambda=0.01$, $L/\lambda=0.3$ and $s/\lambda=1$). (a) magnitude of t -directed current, (b) phase of t -directed current.

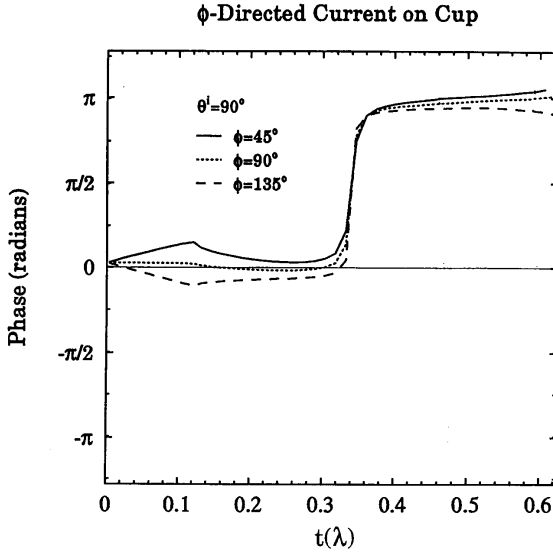
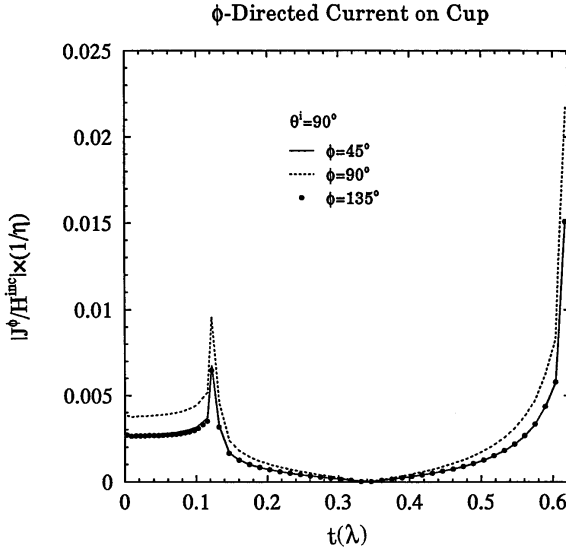


Figure 5. Current distribution on a cup near a wire due to an incident plane wave ($a/\lambda=0.125$, $H/\lambda=0.5$, $b/\lambda=0.01$, $L/\lambda=0.3$ and $s/\lambda=1$). (c) magnitude of ϕ -directed current, (d) phase of ϕ -directed current.

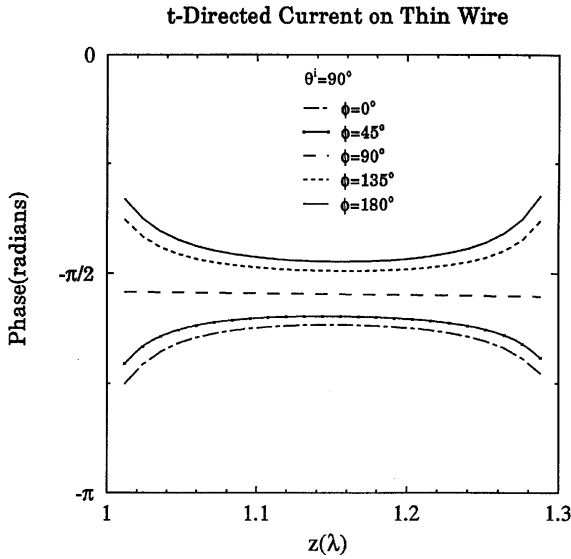
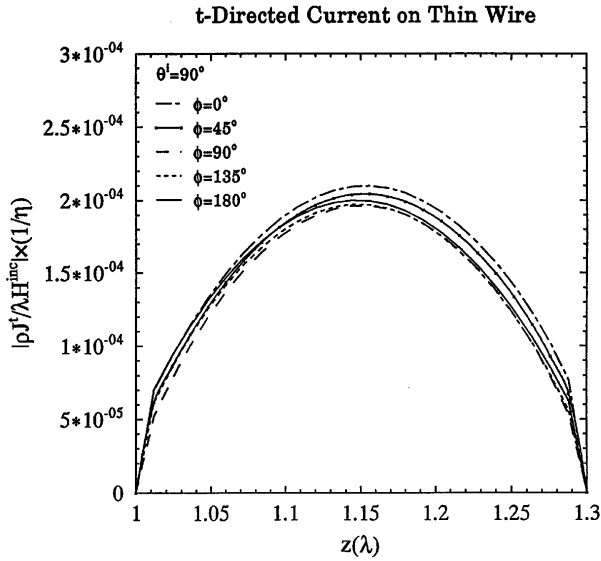


Figure 6. Current distribution on a thin wire near a cup due to an incident plane wave ($a/\lambda=0.125$, $H/\lambda=0.5$, $b/\lambda=0.01$, $L/\lambda=0.3$ and $s/\lambda=1$). (a) magnitude of t -directed current, (b) phase of t -directed current.

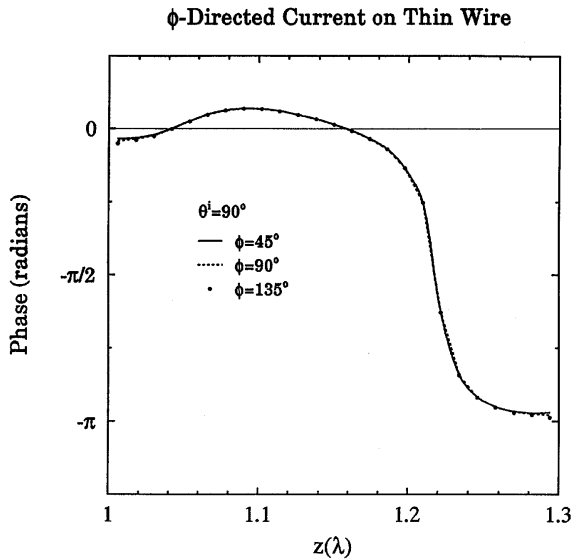
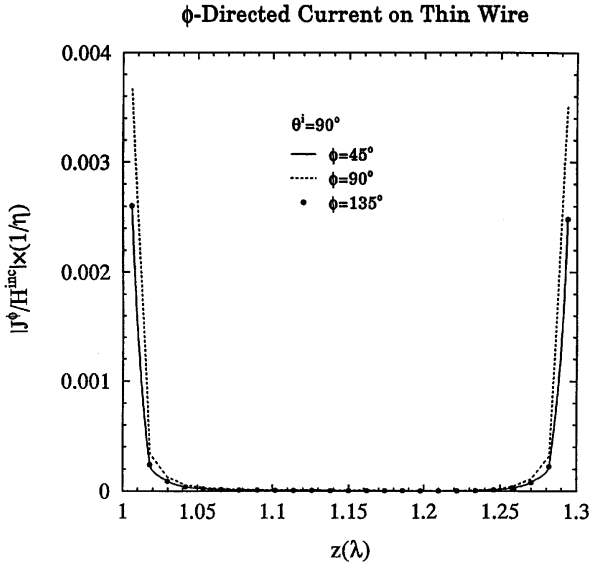


Figure 6. Current distribution on a thin wire near a cup due to an incident plane wave ($a/\lambda=0.125$, $H/\lambda=0.5$, $b/\lambda=0.01$, $L/\lambda=0.3$ and $s/\lambda=1$). (c) magnitude of ϕ -directed current, (d) phase of ϕ -directed current.

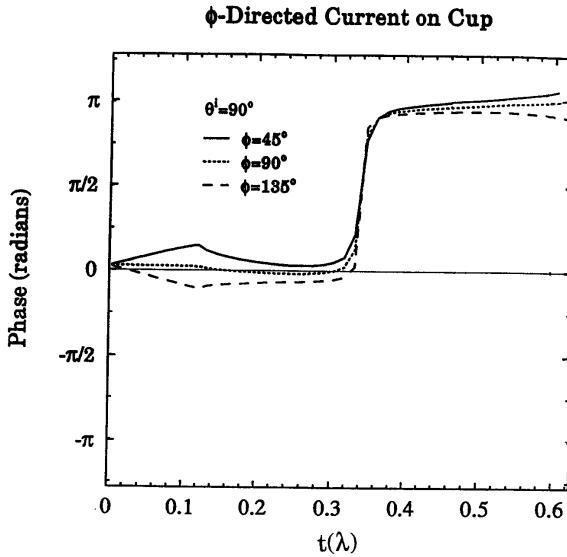
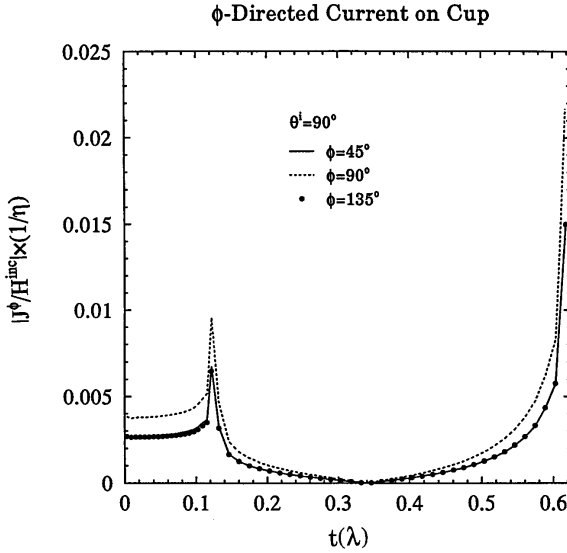


Figure 7. Current distribution on a cup near a wire due to an incident plane wave ($a/\lambda=0.125$, $H/\lambda=0.5$, $b/\lambda=0.01$, $L/\lambda=0.3$, and $s/\lambda=0.35$). (c) magnitude of ϕ -directed current, (d) phase of ϕ -directed current.

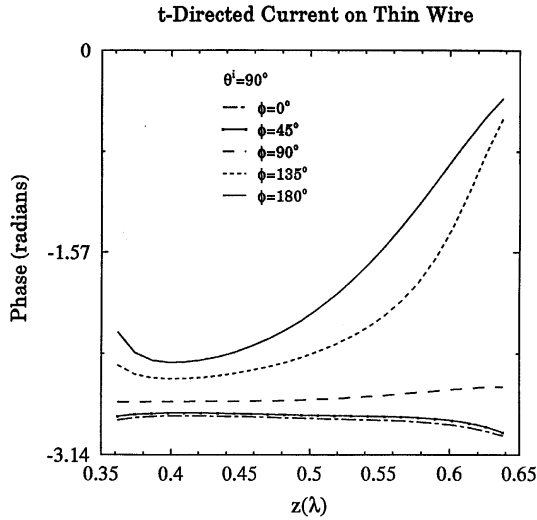
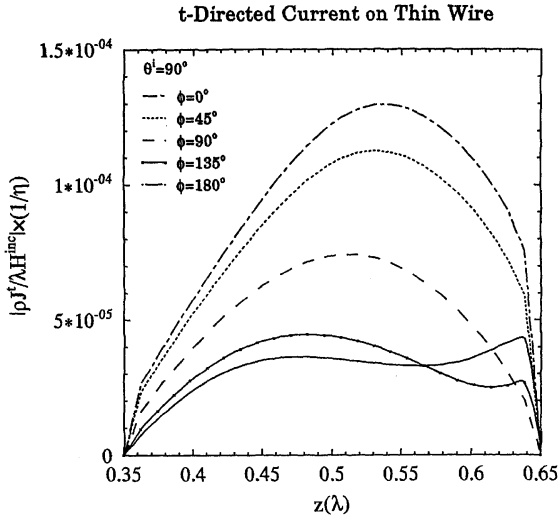


Figure 8. Current distribution on a thin wire near a cup due to an incident plane wave ($a/\lambda=0.125$, $H/\lambda=0.5$, $b/\lambda=0.01$, $L/\lambda=0.3$ and $s/\lambda=0.35$). (a) magnitude of t -directed current, (b) phase of t -directed current.

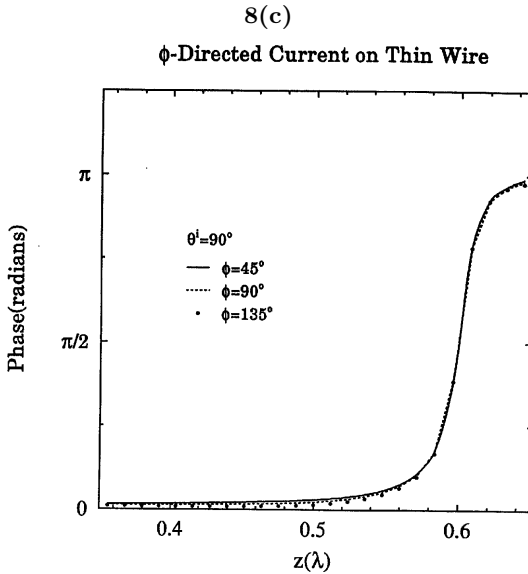
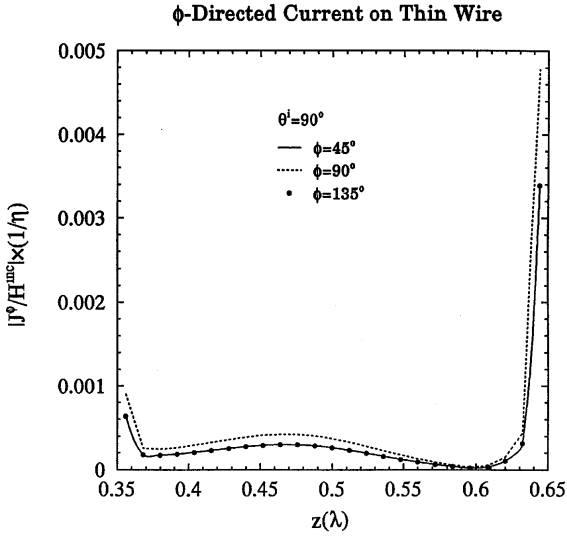


Figure 8. Current distribution on a thin wire near a cup due to an incident plane wave ($a/\lambda=0.125$, $H/\lambda=0.5$, $b/\lambda=0.01$, $L/\lambda=0.3$ and $s/\lambda=0.35$). (c) magnitude of ϕ -directed current, (d) phase of ϕ -directed current.

For the special case in which the wire is a monopole (antenna) mounted on and driven against a finite-length cylinder end cap, erected over a ground plane (Figure 9), the reflection coefficient at the end cap-wire junction is obtained and presented in Figure 10. Γ is determined experimentally in order to corroborate the theoretical results. In the experimental model, the antenna is the extended center conductor of an 0.085 mil semi-rigid coax which is fed through an access hole in the ground plane. Measurements were made with an HP8510B network analyzer. The input admittance at the base (coax aperture) is obtained from the theory and from measured data. Good agreement between the measured and numerical results is observed in Figure 11.

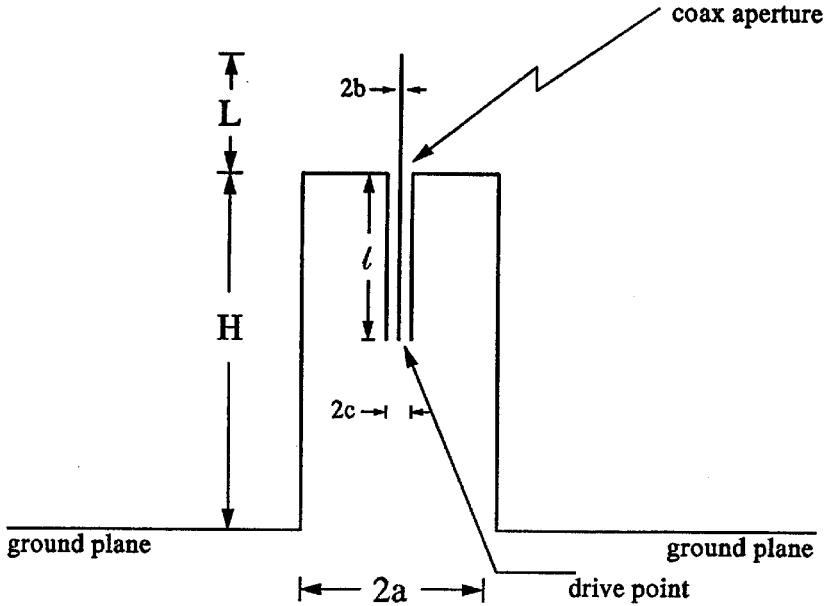


Figure 9. A cross-sectional view of a coax-fed wire antenna mounted on the upper cap of a finite-length cylinder, erected over a ground a plane. Tube $2a = 5.085\text{cm}$ $H = 16.554\text{cm}$ Wire $L = 5.222\text{cm}$ $2b = 0.0912\text{cm}$ $2c = 0.29845\text{cm}$ $l = 26.27\text{cm}$

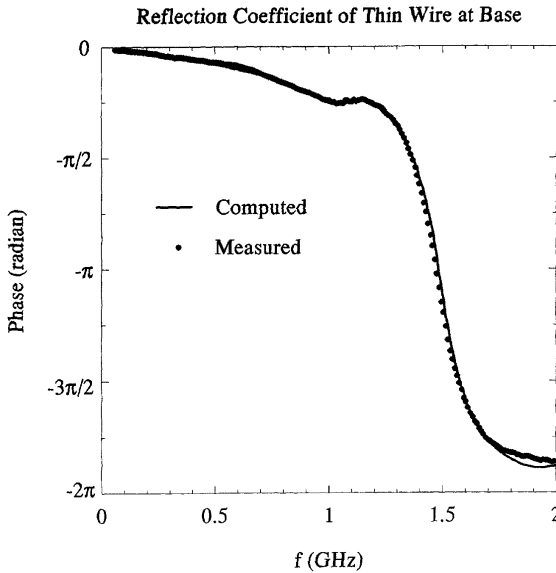
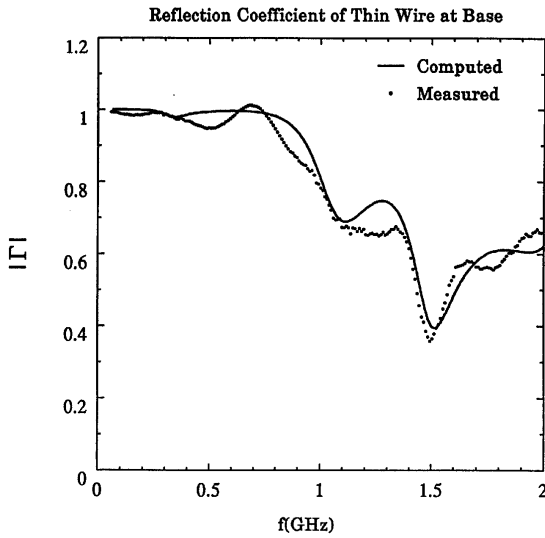


Figure 10. Reflection coefficient at the base of a thin wire monopole antenna on a capped cylinder ($2a=5.085\text{cm}$, $H=16.554\text{cm}$, $L=5.222\text{cm}$, $2b=0.0912\text{cm}$ and $2c=0.29845\text{cm}$). (a) magnitude, (b) phase.

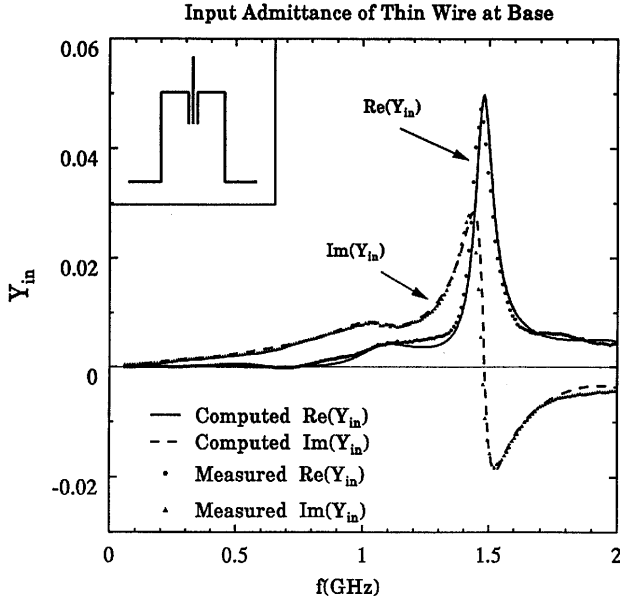


Figure 11. Input Admittance at the base of a thin wire monopole antenna on a capped cylinder($2a = 5.085\text{cm}$, $H = 16.554\text{cm}$, $L = 5.222\text{cm}$, $2b = 0.0912\text{cm}$ and $2c = 0.29845\text{cm}$). Tube $2a = 5.085\text{cm}$ $H = 16.554\text{cm}$ Wire $L = 5.222\text{cm}$ $2b = 0.0912\text{cm}$ $2c = 0.29845\text{cm}$

The current on a “shielded” wire antenna is depicted in Figure 12. The wire is on the axis of a “capped cup” and extends through a circular hole in the cup’s upper end cap as suggested in cross-section in the insert of Figure 12. The antenna, which is of total length $L = 0.75\lambda$ and radius $b = 0.001\lambda$, is driven at its base against the interior surface of the cup’s lower end cap. The total height of the cup is $H = 0.5\lambda$ and its radius is $a = 0.125\lambda$. The diameter of the hole in the upper end cap is $d = 2a_1 = 0.125\lambda$. In Figure 12 are shown values of the t -directed electric current on the thin-wire antenna and on the cup due to a one-volt slice generator. To read the values of current from Figure 12, at points on the structure, one begins at $t = 0$ at the top end of the exposed wire where the current is zero, proceeds downward in the direction of positive t displacement to the point where the wire is driven against the interior side of the cup bottom, moves radially

outward on the cup bottom, then up to the upper cap, and finally inward on the cup cap to the edge of its hole where the current is again zero. Even though only one-third of the wire is not shielded by the cup, substantial radiation takes place as one infers from the observation that the real part of the current is significant (actually large) compared to the imaginary part.

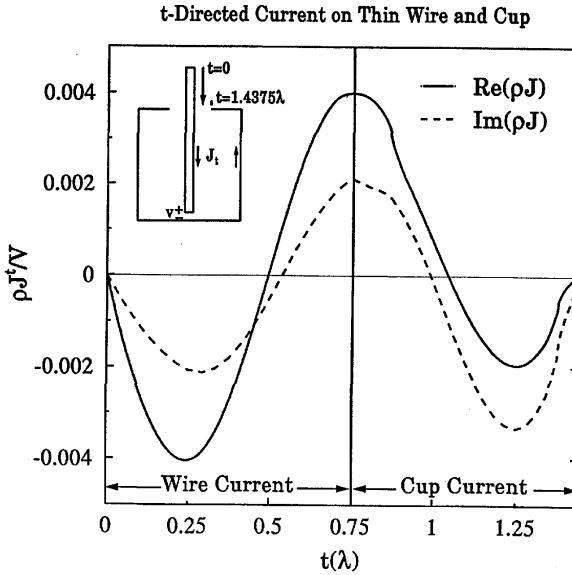


Figure 12. t -directed current on a thin wire and a cup, fed where the wire and cup join ($2a/\lambda=0.25$, $2a_1/\lambda=0.125$, $H/\lambda=0.5$, $b/\lambda=0.001$ and $L/\lambda=0.75$). Cup: $2a=0.25\lambda$ $2a_1=0.125\lambda$ $H=0.5\lambda$ Wire: $b=0.001\lambda$ $L=0.75\lambda$

Appendix A: Bor Integral Equations

The boundary condition that the tangential component of the total electric field is zero on the surface of body can be stated through the use of the following equations,

$$\begin{aligned}
 & j\frac{\eta}{k} \left\{ k^2 \int_0^T \int_{-\pi}^{\pi} (J_t(t', \phi') \hat{t}' \cdot \hat{t} + J_\phi(t', \phi') \hat{\phi}' \cdot \hat{t}) G(t, \phi; t', \phi') \rho' d\phi' dt' \right. \\
 & \left. + \frac{\delta}{\delta t} \int_0^T \int_{-\pi}^{\pi} \left[\frac{\delta}{\delta t'} (\rho' J_t(t', \phi')) + \frac{\delta}{\delta \phi'} J_\phi(t', \phi') \right] G(t, \phi; t', \phi') d\phi' dt' \right\} \\
 = & - E_t^i(t, \phi) \tag{12}
 \end{aligned}$$

$$\begin{aligned}
 & - j\frac{\eta}{k} \left\{ k^2 \int_0^T \int_{-\pi}^{\pi} \left[J_t(t', \phi') \hat{t}' \cdot \hat{\phi} + J_\phi(t', \phi') \hat{\phi}' \cdot \hat{\phi} \right] G(t, \phi; t', \phi') \rho' d\phi' dt' \right. \\
 & \left. + \frac{1}{\rho} \frac{\delta}{\delta \phi} \int_0^T \int_{-\pi}^{\pi} \left[\frac{\delta}{\delta t'} (\rho' J_t(t', \phi')) + \frac{\delta}{\delta \phi'} J_\phi(t', \phi') \right] G(t, \phi; t', \phi') d\phi' dt' \right\} \\
 = & - E_\phi^i(t, \phi) \tag{13}
 \end{aligned}$$

where \hat{t} and $\hat{\phi}$ are the unit tangent vectors on the surface of the body along the generating arc as suggested in Figure 1. t is arc displacement from a reference at $t = 0$ along the generating arc.

In Eqs. (12) and (13), we note that the unknown t -directed (J_t) and ϕ -directed (J_ϕ) electric currents both depend on position (t, ϕ) on the surface S on which the two equations are enforced. In general, it is very difficult and time-consuming to solve these two coupled integral equations in two variables. However, by taking advantage of the ϕ -symmetry of the BOR, one can expand all terms in the two equations in Fourier series. The two coupled integral equations for the unknown electric current components can then be simplified to equations for the Fourier coefficients of the electric current components which depend on only t :

$$\begin{aligned}
 & - j2\pi \frac{\eta}{k} \left\{ k^2 \left[(\cos \gamma \cos \gamma' G_m(t; t') J_m^t(t') \right. \right. \\
 & \left. \left. + \frac{1}{2} \sin \gamma \sin \gamma' (G_{m+1}(t; t') + G_{m-1}(t; t')) J_m^t(t') \right. \right. \\
 & \left. \left. + j\frac{1}{2} \sin \gamma (G_{m+1}(t; t') - G_{m-1}(t; t')) J_m^\phi(t') \right] \rho' dt' \right\} \tag{14}
 \end{aligned}$$

$$+ \left\{ \left[\frac{d}{dt'} \left(\rho' J_m^t(t') \right) + jm J_m^\phi(t') \right] G_m(t; t') dt' \right\} = -E_m^t(t), \quad t \in (0, T)$$

and

$$\begin{aligned} & jk\pi \left\{ k^2 \left[-j \sin \gamma' \left(G_{m+1}(t; t') - G_{m-1}(t; t') \right) J_m^t(t') \right. \right. \\ & \left. \left. + \left(G_{m+1}(t; t') + G_{m-1}(t; t') \right) J_m^\phi(t') \right] \rho' dt' \right. \\ & \left. + jm \frac{2}{\rho} \left[\left(\rho' J_m^t(t') \right) + jm J_m^\phi(t') \right] G_m(t; t') dt' \right\} = -E_m^\phi(t), \quad t \in (0, T) \end{aligned} \quad (15)$$

J_m^t and J_m^ϕ are the m th order Fourier coefficients of J_t and J_ϕ

$$J_m^p(t') = \frac{1}{2\pi} J_p d\phi', \quad (16)$$

where p represents t or ϕ . The m th coefficient of the Green's function is given by

$$G_m = \frac{1}{2\pi} \cos m\zeta d\zeta \quad (17)$$

where $R = \left[\rho^2 + \rho'^2 - 2\rho\rho' \cos \zeta + (z - z')^2 \right]^{1/2}$, and the m th coefficient of the electric field of the incident plane wave is computed from

$$E_m^p = \frac{1}{2\pi} E_p^i e^{-jm\phi} d\phi. \quad (18)$$

Acknowledgements

The authors gratefully acknowledge support of this work by the U.S. Army Research Office through Grant DAAL 03-92-G-0376. Also, the encouragement and support of Ms. Joy L. Arthur and Dr. Glenn L. Brown are sincerely appreciated.

References

1. Glisson, A. W., and C. M. Butler, "Analysis of a wire in the presence of a body of revolution," *IEEE Trans. Antennas and Propagat.*, Vol. AP- 28, 604–609, Sept. 1980.
2. Newman, E. H., and D. M. Pozar, "Electromagnetic modeling of composite wire and surface geometries," *IEEE Trans. Antennas and Propagat.*, Vol. AP- 26, 784–789, Nov. 1978.
3. Shaeffer, J. F., and L. N. Medgyesi-Mitschang, "Radiation from wire antenna attached to bodies of revolution: the junction problem," *IEEE Trans. Antennas and Propagat.*, Vol. AP- 29, 479–487, May 1981.
4. Shaeffer, J. F., "EM scattering from bodies of revolution with attached wires," *IEEE Trans. Antennas and Propagat.*, Vol. AP- 30, 426–431, May 1982.
5. Richmond, J. H., "Monopole antenna on circular disk," *IEEE Trans. Antennas and Propagat.*, Vol. AP- 32, 1282–1287, Dec. 1984.
6. Perez-Leal, R., and M. F. Catedra, "Input impedance of wire antennas attached on-axis to conducting bodies of revolution," *IEEE Trans. Antennas and Propagat.*, Vol. AP- 36, 1236–1243, Sept. 1988.
7. Tsai, L. L., "Dipole antenna coaxially mounted on a conducting cylinder," *IEEE Trans. Antennas and Propagat.*, Vol. AP- 20, 89–94, Jan. 1973.
8. Yung, E. K., and C. M. Butler, "Electrically thick conducting cylinder over a ground plane," *IEE Proceedings*, Vol. 131, 54–60, Feb. 1984.
9. Weiner, M. M., "Monopole element at the center of a circular ground plane whose radius is small or comparable to a wavelength," *IEEE Trans. Antennas and Propagat.*, Vol. AP-35, 488–495, May 1987.
10. Marin, M., and M. F. Catedra, "A study of monopole arbitrarily located on a disk using hybrid MM/GTD techniques," *IEEE Trans. Antennas and Propagat.*, Vol. AP- 35, 287–292, Mar. 1987.
11. Butler, C. M., and L. L. Tsai, "An alternate frill field formulation," *IEEE Trans. Antennas and Propagat.*, Vol. AP-21, 115–116, Jan. 1973.

12. Butler, C. M., A. Q. Martin, and K. A. Michalski, "Analysis of a cylindrical antenna in a circular aperture in a screen," *Journal of Electromagnetic Waves and Applications*, Vol. 8, No. 2, 149–173, 1994.